Dual Masking of Specific Negative Splicing Regulatory Elements Resulted in Maximal Exon 7 Inclusion of *SMN2* Gene

Peng Wen Pao[1], Keng Boon Wee[2], Woon Chee Yee[1] and Zacharias Aloysius DwiPramono[3]

[1]*Formerly Department of Clinical Research, Singapore General Hospital, Singapore, Singapore;* [2]*A*STAR Institute of High Performance Computing, Singapore, Singapore;* [3]*Department of Research, National Skin Centre, Singapore, Singapore.*

Spinal muscular atrophy (SMA) is a fatal autosomal recessive disease caused by survival motor neuron (SMN) protein insufficiency due to *SMN1* mutations. Boosting *SMN2* expression is a potential therapy for SMA. *SMN2* has identical coding sequence as *SMN1* except for a silent C-to-T transition at the 6th nucleotide of exon 7, converting a splicing enhancer to a silencer motif. Consequently, most *SMN2* transcripts lack exon 7. More than ten putative splicing regulatory elements (SREs) were reported to regulate exon 7 splicing. To investigate the relative strength of each negative SRE in inhibiting exon 7 inclusion, antisense oligonucleotides (AONs) were used to mask each element, and the fold increase of full-length *SMN* transcripts containing exon 7 were compared. The most potent negative SREs are at intron 7 (in descending order): ISS-N1, 3′ splice site of exon 8 (ex8 3′ss) and ISS+100. Dual-targeting AONs were subsequently used to mask two nonadjacent SREs simultaneously. Notably, masking of both ISS-N1 and ex8 3′ss induced the highest fold increase of full-length *SMN* transcripts and proteins. Therefore, efforts should be directed towards the two elements simultaneously for the development of optimal AONs for SMA therapy.

Received 25 July 2013; accepted 1 December 2013; advance online publication 28 January 2014. doi:10.1038/mt.2013.276

INTRODUCTION

Spinal muscular atrophy (SMA) is characterized by progressive voluntary muscle atrophy resulting from the degeneration of α-motor neurons in the anterior horns of the spinal cord. This is due to insufficient amount of survival motor neuron (SMN) protein which is expressed primarily by *SMN1* but is mutated in SMA patients, and marginally by *SMN2* genes.[1] Both genes are mapped to Chromosome 5q13 as inverted repeats whose 1.7 kb full-length cDNAs are identical except for a silent C-to-T transition at the 6th nucleotide (C6T) of *SMN2*'s exon 7,[2] and another one at exon 8. The transition converts the SF2/ASF splicing factor-specific exonic splicing enhancer (ESE) motif to a heterogeneous nuclear ribonucleoprotein (hnRNP) A1 repressor protein-specific exonic splicing silencer (ESS) motif, and generates an extended inhibitory context against exon 7 retention.[3–5] Generally, ~90% of *SMN2* mRNA transcripts lack exon 7 whose truncated gene products are unstable and nonfunctional.[6] As SMA patients retain at least one copy of *SMN2*, the expression of full-length *SMN* transcripts can be restored by correcting aberrant exon 7 splicing. The plausibility of this strategy to reverse or ameliorate the phenotype is supported from clinical observations that phenotype severity correlates inversely with *SMN2* copy number;[7–9] more *SMN2* copies suggests more endogenous full-length *SMN* transcripts and thus larger compensatory effect.

The regulation of *SMN2* exon 7 splicing involves more than 10 putative splicing regulatory elements (SREs) located from intron 6 to exon 8 (**Figure 1**). They encompass four positive SREs (enhance exon 7 inclusion; shaded in gray), six negative SREs (inhibit exon 7 inclusion; shaded in black), and splice sites of which the latter two are of particular relevance for the induction of exon 7 inclusion. In the case of negative SREs, two are at intron 6 (Element 1 and a putative one downstream of Element 1), two are at exon 7 (ESS A and ESS B), two at intron 7 (ISS-N1 and ISS+100). Both the splice sites at exon 7's 5′ and exon 8 3′ are hypothesized to inhibit exon 7 inclusion. The proposed terminal stem loop 2 (TSL2) nascent mRNA structure at the former was hypothesized to inhibit U1 snRNP from binding to the splice site and subsequent exon 7 processing.[10] The latter splice site was proposed to compete with 3′ splice site of exon 7 in joining to 5′ splice site of exon 6 during splicing.[11] Exon 8 was hypothesized to be preferentially paired with exon 6 as the C6T transition, proposed TSL2 and exon 7's weak splice sites[6] contributed to the attenuation of splicing factors' affinity towards exon 7. Refer to **Figure 1** legend for more details.

The regulation of SRE on exon 7 splicing can be validated by masking the element via antisense oligonucleotides (AONs) as steric hindrance between the SRE and its associated regulatory protein(s).[12,13] Indeed, AONs masking positive SREs augmented exon 7 skipping whereas the converse was observed for AONs masking either negative SREs or 3′ splice site of exon 8; AON target sites depicted in **Figure 1**. With the list of reported SREs, it is natural to ask the following questions in the context of applying AON as a possible therapy for SMA. What is the relative importance of each negative SRE in inhibiting exon 7 inclusion? That is, is it possible to differentiate critical SREs from noncritical or

Correspondence: W.C.Y. who passed away on 31 August 2011 contributed significantly to this study. Zacharias Aloysius DwiPramono, National Skin Centre, 1 Mandalay Road, Singapore 308205, Singapore. E-mail: dpsarengat@nsc.gov.sg

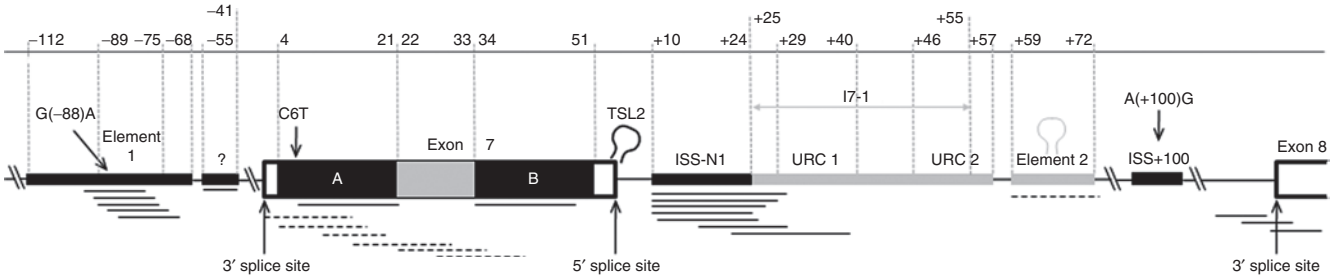

Figure 1 Positive and negative splicing regulatory elements (SREs) modulating SMN2 exon 7 splicing. *SMN2* gene depicted from part of intron 6 to partial exon 8 (not drawn to scale). Positive SREs which promotes exon 7 inclusion are shaded in gray whereas negative SREs which inhibit exon 7 inclusion are shaded in black. Published antisense oligonucleotide (AON) target sites are indicated as either full (augmented exon 7 retention) or broken (induced exon 7 skipping) lines below the gene; Element 1,[25,42] putative ISS at intron 6,[43] exonic splicing silencer (ESS) A,[12] exonic splicing enhancer (ESE) at exon 7,[12,13] ESS B,[12] ISS-N1,[13,19–24] URC1,[19] Element 2,[18] and 3′ splice site of exon 8.[11,14,44] The relative positions of the polymorphisms are indicated. Numbering of nucleotide position is relative from the first nucleotide: at 3′ of exon 7 in both intron 6 and exon 7, and at 3′ of intron 7 in intron 7 ("+" is appended to differentiate it from exonic sequence). Positive SREs: The exonic positive SRE, which is contiguously flanked by two splicing silencer elements, has been reported to be associated with several serine-rich (SR) or SR-like proteins including Tra2β1, SRp30c, RBMY, and hnRNP-G.[12,27–29] Correspondingly, antisense oligonucleotides (AONs) bound to this element (depicted as dashed lines) further enhanced exon 7 exclusion in *SMN2* transcripts. On the other hand, the three intronic positive SREs are clustered together. Two U-rich clusters (URC1 and URC2) have been reported to be TIA1 binding sites which recruits U1 snRNP needed for splicing.[26] Both URC1 and URC2 motifs overlap with I7-1, a 31 nt-segment reported to promote exon 7 inclusion.[31] Element 2 was found to be critical for exon 7 inclusion where its stem-loop RNA structure is required to recruit an unidentified splicing protein.[18] Indeed, an AON bound to Element 2 promoted exon 7 skipping. Negative SREs: ESSs A and B sandwich the lone positive SRE in exon 7.[12] Notably, the C6T transition that occurred within ESS A augments hnRNP A1 binding.[4] Element 1, located at intron 6 that encompassed the G(-88)A transition, was reported to be binding sites for hnRNP1 and FUSEBP.[25,42] A putative negative SRE was also reported at intron 6 downstream of Element 1.[13] Lastly, the remaining two negative SREs, ISS-N1 and ISS+100, flanked all the three intronic positive SREs at intron 7. In fact, ISS-N1 consisted of two weak hnRNAP A1/A2 motifs[19] that cooperate to make up a strong splicing inhibitory effect.[13] The A(+100) G transition generated a silencer motif at ISS+100 and was reported to have high affinity towards hnRNP A1.[33]

redundant ones? This cannot be inferred readily from prior studies wherein not more than two elements were compared at a time, and due to the use of different cell lines (with varying *SMN2* copy number) or *SMN2* minigenes of varying length, and different AON chemistry and concentration. Furthermore, not all negative SREs were targeted (*e.g.*, ISS+100). In addition, are the inhibitory effects on exon 7 inclusion from the various negative SREs cooperative or additive? Both effects have not been observed thus far in *SMN2* exon 7 splicing regulation.[14]

Three aims were attempted. First, novel AONs were designed rationally to mask each intronic SRE and 3′ splice site of exon 8 optimally. Second, the extent of full-length *SMN* transcripts induced upon masking each negative SRE (intronic and exonic) or 3′ splice site of exon 8 was measured under identical experimental system and compared. Third, dual-targeting AONs, in which an AON masks two nonadjacent SREs simultaneously, were used to infer possible cooperative or additive effects among SREs. Notably, the dual masking of ISS-N1 and 3′ splice site of exon 8 resulted in the highest fold increase in full-length *SMN* transcripts over all tested single- or dual masking of other elements, which suggests they are the most important SREs to mask for maximizing the expression of full-length *SMN* transcripts for SMA therapy.

RESULTS

Design of AONs to mask intronic negative SREs and 3′ splice site of exon 8

9 novel AONs were synthesized to mask Element 1, ISS-N1, ISS+100 or 3′ splice site of exon 8 (**Table 1**). The target sites were rationally selected for optimal AON binding by taking into consideration the accessibility of cotranscriptional secondary structures of the nascent mRNA, and favorable biophysical and thermodynamic properties of the binding of the AON and target site, as described previously.[15,16] A minimum target length of 17 nucleotides was chosen as an additional criterion to minimize unspecific binding to the human genome. Note that ISS+100 have not been targeted by AON.

Comparative study of AONs in inducing full-length SMN transcripts

For comparison as well as positive controls, AONs were also synthesized for previously published target sites that were shown to be effective in mediating full-length *SMN* transcripts production (**Table 1**). For negative controls, a scrambled AON and Lipofectamine2000 only were used. All AONs were synthesized with 2′-O-methyl and phosphorothioate backbone modifications and were transfected at 100 nmol/l into GM03813 cells[17] (primary cultures of fibroblast cells derived from a Type I SMA patient, $SMN1^{-/-}$). Their efficacy was determined by reverse transcription-PCR analysis and followed by bidirectional sequencing analysis to confirm exon 7 inclusion in *SMN* transcripts. Their efficiency was estimated by densitometry of the gel electrophoresis images that semiquantified the amplicons with or without exon 7. AON efficiency is presented as a percentage of the amplicon copies with exon 7 to total amplicon copies. **Figure 2a** shows the raw gel electrophoresis data of RT-PCR products from efficient AONs that can induce high level of exon 7 inclusion. The ImageJ analysis of the same data presenting the AON efficiencies is given in **Figure 2b**. Notably, the masking of each negative SRE at intron 6 or at exon 7 was less effective in inducing exon 7 inclusion (**Supplementary Figure S1**) than the masking of each of the three SREs at intron 7 (ISS-N1, ISS+100 and 3′ splice site of exon 8).

To investigate the relative strength of the negative SREs at intron 7, efficient AONs masking these elements were further tested at various AON transfection concentrations using qRT-PCR.

Table 1 List of novel and published single-targeting AONs tested in this study

SRE	AON	Target site relative position (3′–5′)	Target length	AON sequence (5′–3′)
Element 1	E1-1	−105 to −81	25	UAAAAAGCAUUUUGUUUCACAAGAC
	E1-2	−97 to −73	25	AUGGAUGUUAAAAAGUAUUUUGUUU
	E1-Miy[42]	−89 to −74	16	UGGAUGUUAAAAAGUA
ESSA	ESSA-Hua[12]	7 to 21	15	UUUUUGAUUUUGUCU
ESSB	ESSB-Hua[12]	34 to 48	15	AUUUAAGGAAUGUGA
ISS-N1	N1-1	+8 to +29	22	AUUCACUUUCAUAAUGCUGGCA
	N1-2	+9 to +29	21	AUUCACUUUCAUAAUGCUGGC
	N1-3	+9 to +30	22	GAUUCACUUUCAUAAUGCUGGC
	N1-4	+10 to +30	21	GAUUCACUUUCAUAAUGCUGG
	N1-Singh[19,20]	+10 to +29	20	AUUCACUUUCAUAAUGCUGG
	N1-Hua[13,22,23]	+10 to +27	18	UCACUUUCAUAAUGCUGG
ISS+100	+100–1	+95 to +113	19	ACCUUUCAACUUUCUAACA
3′ splice site of exon 8	ex8-1	−13 to 5	18	AUUUCCUGCAAAUGAGAA
	ex8-2	−5 to 12	17	UGCCAGCAUUUCCUGCA
	ex8-Lim[11,14]	−11 to 10	21	CUAGUAUUUCCUGCAAAUGAG

AON target site's position is relative from the first nucleotide: at 3′ of exon 7 in both intron 6 and exon 7, at 3′ of intron 7 with "+" appended in intron 7, and at 3′ of exon 8 in 3′ splice site of exon 8.
AON, antisense oligonucleotide; ESS, exonic splicing silencer; SREs, splicing regulatory elements.

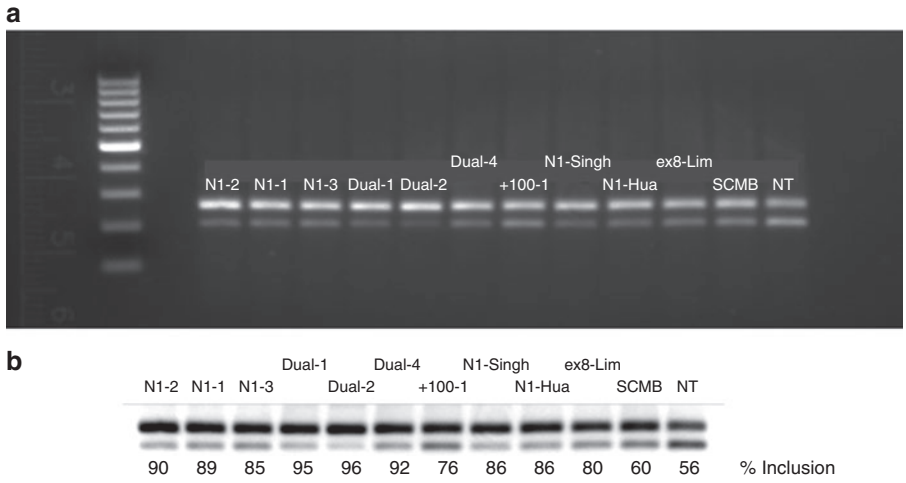

Figure 2 Gel electrophoresis images of *SMN* amplicons. (**a**) RT-PCR products were amplified using forward primer at exon 6 and reverse primer at exon 8. Bands: upper: amplicons with exon 7; lower: amplicons without exon 7. SCRM: scrambled AON. NC: negative control where cells were transfected with Lipofectamine 2000 only. Lane labels prefixed with "Dual" refer to dual-targeting AONs (see text below). (**b**) The same gel electrophoresis image with inverted color. The efficiency of each AON in inducing exon 7 inclusion, measured by densitometer comparing upper band and lower band, are presented in % under each corresponding lane. AON, antisense oligonucleotide.

The fold increase (of exon 7 inclusion) induced by each AON was normalized with the internal control (GAPDH) and the data was further normalized to the level of the corresponding transcript in the normal control (Lipofectamine2000 only; labeled as NT). For each AON, duplicate transfections were performed each at the concentration of 25 nmol/l, 50 nmol/l, 100 nmol/l, and 200 nmol/l, followed by triplicates of qRT-PCR analyses per AON transfection. The mean and standard deviation of fold increase of full-length *SMN* transcripts are plotted in **Figures 3a–d** respectively.

Masking ISS+100 resulted in the highest fold increase of full-length *SMN* transcripts at 200 nmol/l of AON concentration. At lower concentrations, masking ISS-N1 consistently resulted in the highest fold increase while masking 3′ splice site of exon 8 induced similar or higher fold increase than masking ISS+100.

Masking of two negative SREs simultaneously via dual-targeting AONs

As masking ISS-N1, ISS+100, or 3′ splice site of exon 8 was most effective in augmenting exon 7 inclusion, four dual-targeting AONs were synthesized to mask two elements simultaneously. Since ISS-N1 is the most potent element (**Figure 3**), it was targeted in tandem with either ISS+100 or 3′ splice site of exon 8. As

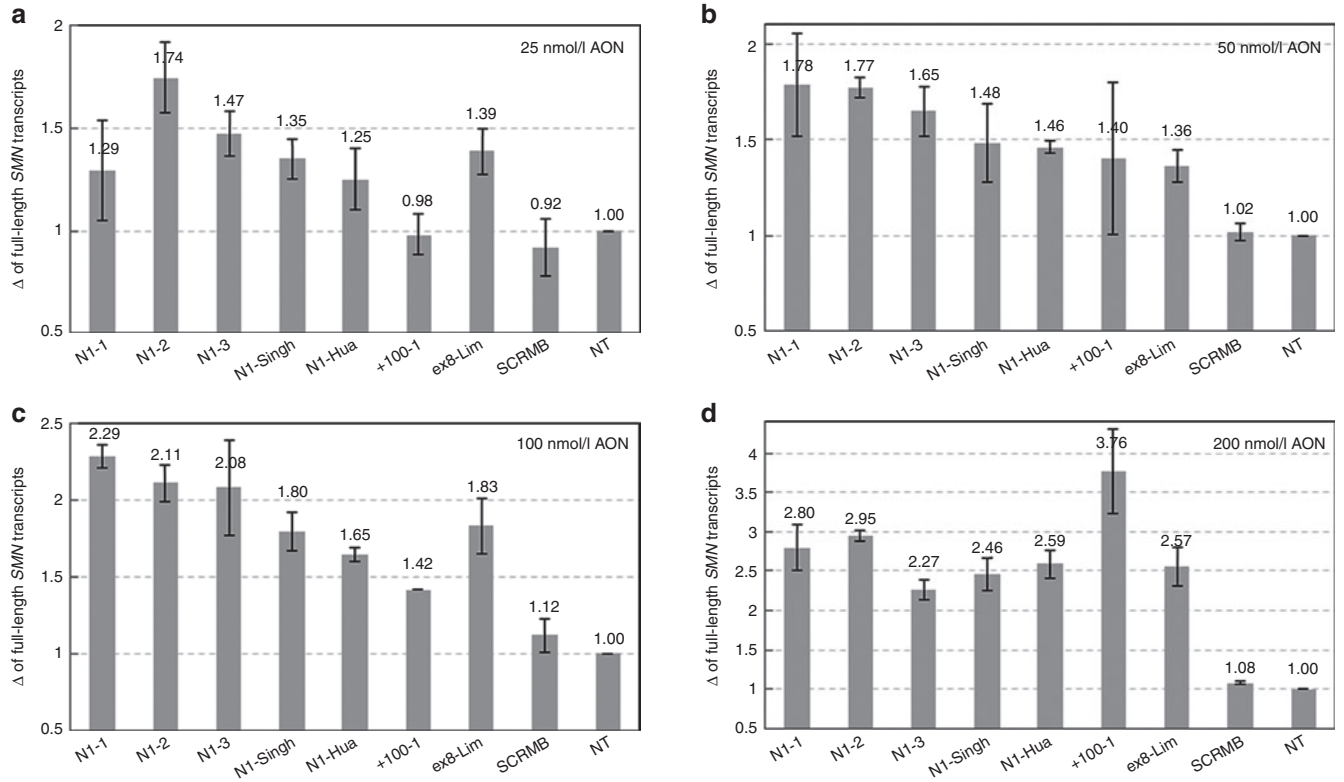

Figure 3 Fold increase of full-length *SMN* transcripts measured at various antisense oligonucleotide (AON) transfection concentrations. (**a**) 25 nmol/l. (**b**) 50 nmol/l. (**c**) 100 nmol/l. (**d**) 200 nmol/l. The fold increase of exon 7 inclusion induced by each AON was normalized with the internal control (GAPDH) and the data was further normalized to the level of the corresponding transcript in the normal control (Lipofectamine2000 only; labeled as NT).

Table 2 List of dual-targeting AONs

SREs	AON	Target sites	Target length
ISS-N1 & 3′ splice site of exon 8	Dual-1	N1-2 & ex8-1	39
	Dual-2	N1-2 & ex8-2	38
	Dual-3	N1-2 & ex8-Lim	42
ISS-N1 & ISS+100	Dual-4	N1-2 & +100–1	40
ESS A & ESS B	Dual-5	ESSA-Hua & ESSB-Hua	30

A dual-targeting AON is single stranded whose continuous sequence is completely complementary to its two target sites.
AON, antisense oligonucleotide; ESS, exonic splicing silencer; SREs, splicing regulatory elements.

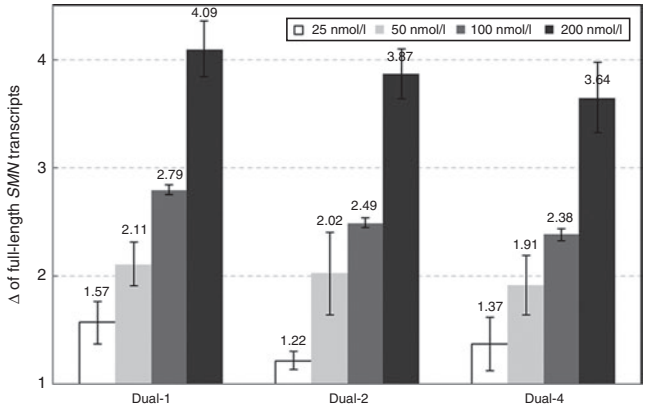

Figure 4 Fold increase of full-length *SMN* transcripts measured at various dual-targeting antisense oligonucleotide (AON) transfection concentrations.

both N1-1 and N1-2 are the most potent AONs targeting ISS-N1 (**Figure 3**), the latter's target site was chosen in the dual-targeting AONs for its shorter sequence. On the other hand, both ex8-1 and ex8-2 were chosen for their shorter sequences whereas ex8-Lim was chosen for its efficiency. **Table 2** tabulates the sequences and their respective target positions of the dual-targeting AONs.

Similarly, the efficiency of the dual-targeting AONs at various AON concentrations was first estimated by densitometry analysis of the RT-PCR products (**Figure 2** and **Supplementary Figure S1**), and subsequently determined by qRT-PCR (**Figure 4**). **Figure 5a** compares the percentage difference in fold increase of full-length *SMN* transcripts induced by Dual-1 (the most efficient dual-targeting AON masking ISS-N1 and 3′ splice site of exon 8) relative to the most efficient single-targeting AONs masking the corresponding elements. Analogously, the performance of Dual-4 was compared with N1-2 and +100–1 (**Figure 5b**); note: at 200 nmol/l of AON dosage, the drastic loss of performance gain of Dual-4 over +100–1 was a result of the substantial increase in the efficiency of the latter (**Figure 3d**), as the efficiency of Dual-4 increases with AON dosage (**Figure 4**). Three observations were discerned. Generally, simultaneous masking of two elements leads to higher fold increase, and that the gain in performance increases with AON dosage. Second, the performance gain of dual masking over separate ISS+100 or 3′ splice site of exon 8 masking was more

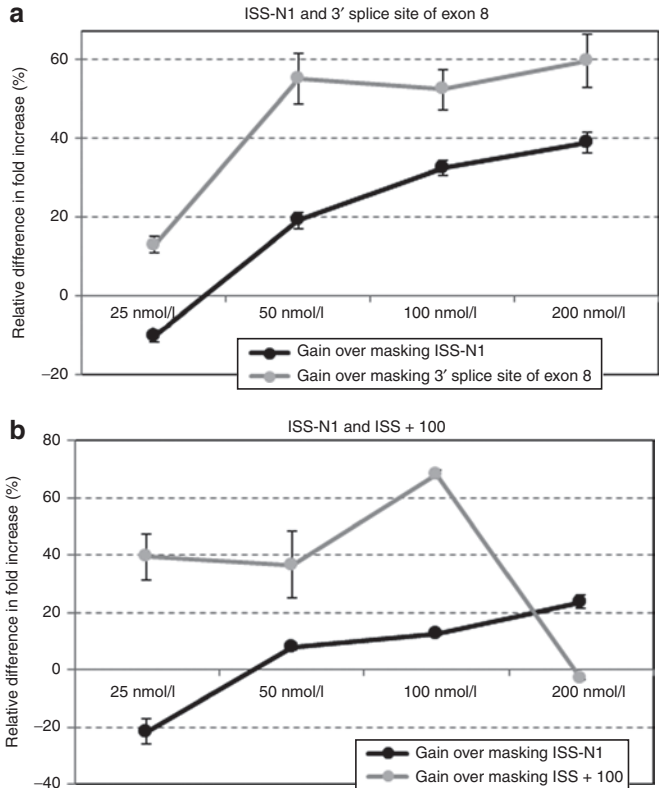

Figure 5 Fold increase of full-length survival motor neuron (SMN) transcripts induced by dual masking as compared to individual masking of two splicing regulatory elements (SREs). Relative percentage difference in fold increase of full-length *SMN* transcript is computed as 100% × Fold increase (Dual – Single)/Fold increase (Single). (**a**) Performance gains of Dual-1 (masking ISS-N1 and 3′ splice site of exon 8) over the most efficient single-masking antisense oligonucleotides (AONs) masking ISS-N1 (N1-2, black) or 3′ splice site of exon 8 (ex8-Lim, gray). (**b**) Performance gains of Dual-4 (masking ISS-N1 and ISS+100) over its single-masking counterparts *i.e.*, N1-2 (black) and +100–1 (gray).

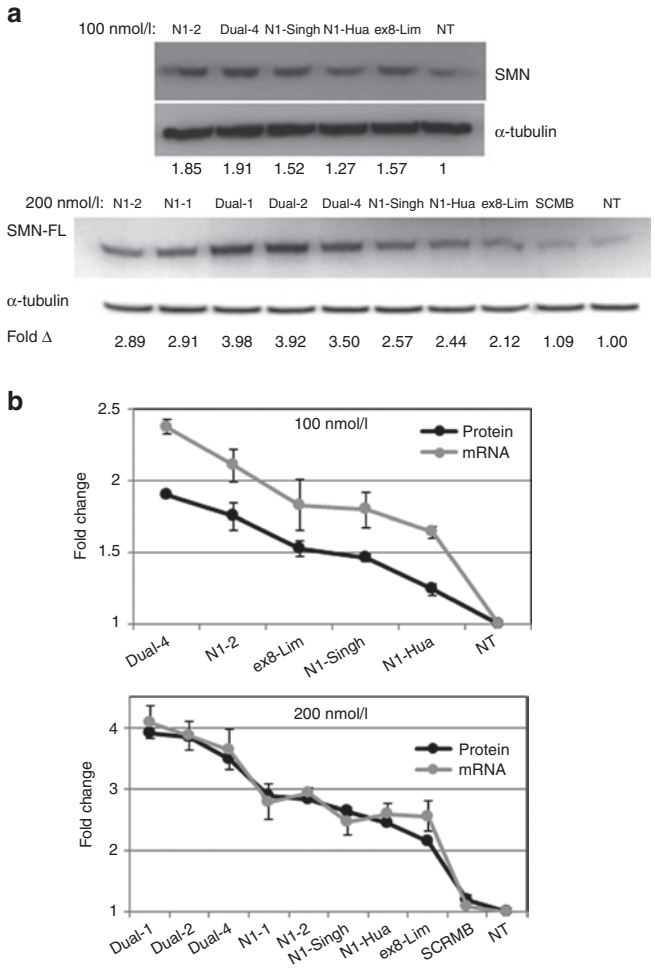

Figure 6 Semiquantitative studies of survival motor neuron (SMN) protein detected upon antisense oligonucleotide (AON) treatment. (**a**) For each AON transfection, duplicates of western blot analyses were performed. The mean fold increase of SMN protein from induced by each AON treatment is relative to Lipofectamine2000 only treatment (denoted as NT). (**b**) Fold increase of full-length *SMN* transcripts (from **Figures 3** and **4**) superimposed with fold increase of full-length SMN protein (from **Figure 6a**) at 100 nmol/l or 200 nmol/l of AON dosage.

than ISS-N1 masking. Third, at low AON dosage (25 nmol/l), dual masking is not more effective than masking only ISS-N1.

Furthermore, Dual-5 was synthesized to mask both ESS A and ESS B (**Table 2**). However, it promoted some exon 7 skipping instead (**Supplementary Figure S1**).

Protein and functional studies

Western blot analyses for SMN protein were performed after incubation with either 100 nmol/l or 200 nmol/l of AON. **Figure 6a** shows the representative results and the mean fold increase of SMN protein detected for various efficient AONs as compared to the untreated control (Lipofectamine2000 only). Notably, the relative efficiency of the AONs in inducing full-length *SMN* transcripts is in accordance with the relative fold increase of protein detected (**Figure 6b**). Hence, the increased full-length *SMN* transcripts resulted in a corresponding upregulation of full-length SMN protein.

The ability of the restored SMN proteins to form nuclear Gemini of coiled bodies (GEMs) was determined in the AON treated cells. The number of nuclear GEMs in each of the 120 consecutive cells, which were stained via immunofluorescence for SMN protein upon treatment with 100 nm of AON, was counted manually. As shown in **Figure 7**, the fraction of cells with GEMs and the number of cells with three or more GEMs both correlate generally with the relative AON efficiency in inducing full-length *SMN* transcripts (**Figure 3** and **Figure 4**). Representative immunofluorescence stained slides for each AON tested in **Figure 7** are given in **Supplementary Figure S2**. For the breakdown of the cell counts with specific numbers of nuclear GEMs induced by each AON, please refer to **Supplementary Figure S3**.

DISCUSSION

By masking negative SREs of the *SMN2* nascent mRNA either separately or in pairs under identical experimental parameters, their relative inhibitory strengths on exon 7 inclusion, which was not addressed in previous studies, can be compared. Six previously reported negative SREs were masked—Element 1 at intron 6, ESS A and ESS B at exon 7, ISS-N1 and ISS+100 at intron 7, and 3′ splice site of exon 8. Each of the 20 novel or previously published efficient AONs targeting the elements was tested for

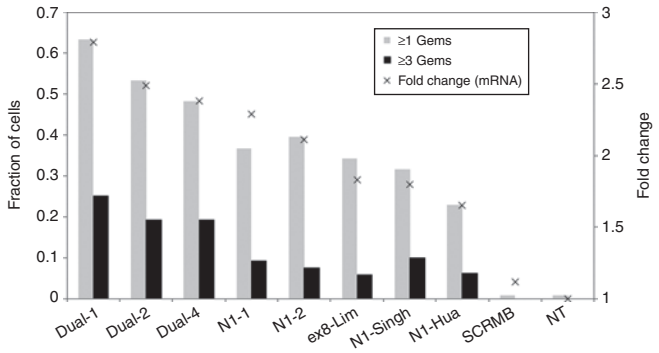

Figure 7 Fraction of cells with GEMs. Fraction of cells observed to have at least one or three nuclear GEMs upon treatment with 100 nmol/l of a specific antisense oligonucleotide (AON) were counted and plotted. A total of 120 cells were used for GEMs counting.

their relative efficiency in augmenting exon 7 inclusion in the mature transcripts. The increased expression of the full-length *SMN* transcripts resulted in a corresponding upregulation of the protein whose ability to form nuclear GEMs in the treated cells was validated. Notably, AON efficiency quantified at the mRNA level generally correlated with the quantity of functional SMN protein measured. Taking the results of the molecular and cellular studies together, masking ISS-N1 and 3′ splice site of exon 8 simultaneously elicited the highest fold increase of full-length *SMN* transcripts and proteins, and highest fraction of cells with nuclear GEMs (**Figures 4**, **6** and **7**). Therefore, efforts should be directed towards the two elements for the development of optimal AONs for SMA therapy.

Intron 7 is considered a regulatory hot spot in exon 7 splicing[18] as it harbors three negative SREs (ISS-N1, ISS+100, and 3′ splice site of exon 8) and three positive SREs (URC1, URC2, and Element 2) (**Figure 1**). While ISS-N1 has been observed to effect strong inhibition on exon 7 inclusion,[13,19–24] the results here indicate that its effect is the strongest (**Figures 3** and **5**). While the relative strength between ISS+100 and 3′ splice site of exon 8 is less marked, the latter seems to be the stronger element—higher fold of full-length *SMN* transcripts was observed when the splice site was masked at low AON dosage (≤100 nmol/l) (**Figure 3**), and higher fold of full-length *SMN* transcripts and proteins, and more cells with nuclear GEMs were observed when the splice site was masked simultaneously with ISS-N1 than when ISS+100 was masked simultaneously with ISS-N1 (**Figures 4**–**7**). AON masking of ISS+100, which has not been reported hitherto, further validates its inhibitory effect on exon 7 inclusion.

Results from this study suggest that negative SREs at either intron 6 (Element 1) or exon 7 (ESS A and ESS B) are less potent (**Supplementary Figure S1**). Masking Element 1 by three different AONs (two novel and one previously published) failed to match the fold increase of full-length *SMN* transcripts induced when either elements in intron 7 or 3′ splice site of exon 8 was masked. The weak inhibitory effect of Element 1 corroborates earlier reports that AONs targeting Element 1 failed to augment full-length *SMN* transcripts,[25] and that TIA1 bound to URC (positive SRE at intron 7; **Figure 1**) can easily counteracts the inhibitory effect of hnRNP 1 bound to Element 1.[26] At exon 7 on the other hand, sandwiching of the ESE by ESS A and ESS B (**Figure 1**) could facilitate steric hindrance between splicing enhancer and inhibitor proteins[27–29] for which the net effect on exon 7 splicing is counterintuitive. For examples, several AONs masking ESS A unexpectedly augmented exon 7 skipping,[12] and as well as Dual-5 that masks ESS A and ESS B simultaneously. Hence, masking negative SREs in exon 7 may not be an optimal therapeutic strategy for the following reasons. An AON annealed to exon 7 may interfere with the protein translation of full-length *SMN2* transcripts in the cytoplasm. Secondly, the sole positive SRE in exon 7 seems to be more critical in mediating exon 7 inclusion than those in intron 7—AONs whose target sites overlapped the ESE and either ESS A or ESS B augmented exon 7 skipping[12,13] whereas target sites overlapping URC1 and ISS-N1 at intron 7 enhanced exon 7 inclusion[19] (**Figure 1**). Due to close proximity, an AON bound to one of the negative SREs may interfere with the recruitment of splicing factors to the ESE, which could be a rate limiting step since Tra2β1 is downregulated in SMA patients.[30] When Dual-5 binds to ESS A and ESS B, it possibly exerts steric hindrance against Tra2β1 recruitment and/or modifies the ESE motif secondary structure to an unfavorable conformation for Tra2β1 binding. Consequently, these factors greatly limit the space for further optimization of AONs. Finally, as a further evidence of the relative weak inhibitory strengths of negative SREs at intron 6 and exon 7, masking Element 1 or ESS A/B together with 3′ splice site of exon 8 failed to improve the fold increase of full-length *SMN* transcripts when only the latter was masked.[14]

Results from prior and current studies showed that simultaneous masking of two negative SREs either by dual-targeting or two separate AONs is not always more effective in inducing full-length *SMN* transcripts. In contrast, simultaneous masking of ISS-N1 and either ISS+100 or 3′ splice site of exon 8 further augmented the fold increase of full-length SMN transcripts and proteins over single masking of each element. The observed magnitudes of the augmentation are substantial which increased with AON dosage generally (**Figure 5**). Hence, this suggests that ISS-N1 albeit the strongest SRE could cooperate with the other two negative SREs, and does not solely dominate the net inhibitory effect on exon 7 inclusion(**Supplementary Figure S4**). This can explain the higher yield of full-length *SMN* transcripts induced from dual over single masking of SREs.

The inclination for ISS-N1 to cooperate with ISS+100 could be due to proximity and also structural arrangements where they enclose three positive SREs (**Figure 1**). That is, through the cooperation of specific proteins recruited to ISS-N1 or ISS+100, they could better counteract the positive SREs possibly by steric hindrance against splicing factors recruited to positive SREs,[13,31,32] or by modifying the higher order structure of the positive SREs to impede recruitment of splicing factors[18,32] such as via the hypothesized loop-out model.[33] On the other hand, masking of ISS-N1 and 3′ splice site of exon 8 simultaneously could promote exon 7 inclusion via two complementary mechanisms – reducing competition from exon 6 in adjoining to exon 8[11,12,24] during the slow kinetics of exon 7 5′ splice site recognition by U1 snRNP,[10,34] and promoting exon 7 recognition by splicing factors through the inhibition of ISS-N1. The observation that higher fold increase of full-length *SMN* transcripts was induced when ISS-N1 is masked together with 3′ splice site of exon 8 than with ISS+100 suggest that the poor definition of *SMN2* exon 7, as a consequence of the C6T transition and the rate limiting recruitment of U1 snRNP to

its 5′ splice site, as the underlying cause of endogenous exon 7 skipping. This could explain why pairing of N1-2 to either ex8-1 or ex8-2, which is not efficient individually (**Supplementary Figure S1**), can significantly augment exon 7 inclusion. Nevertheless, as AON efficiency correlates with target length,[15,16] it is possible that the substantial increase in efficiency when either ex8-1 or ex8-2 is paired to N1-2 could be partially attributed to the extension of the formers' short sequences (≤18 bp).

In this study, a novel strategy in designing AON to mask two nonadjacent SREs simultaneously was explored and was subsequently demonstrated to be effective. The choice of synthesizing a dual-targeting AON over two AONs each masking a specific site is based on the consideration for clinical application. At a given AON dose, a dual-targeting AON can target twice the number of nascent mRNA than two single-targeting AONs; for *e.g.*, 100 nmol/l of dual-targeting AONs is equivalent to 50 nmol/l of each single-targeting AON. Moreover, a dual-targeting AON is shorter (and thus cheaper) than the total length of two single-targeting AONs as the latter must adhered to a minimum length to avoid unspecific binding in the human genome. Although the two target sites of a dual-targeting AON are not adjacent, full complementary binding to the two sites is possible. This is because as the elongating nascent mRNA forms dynamic secondary structures, it can bring nonadjacent local segments of a RNA in proximity.[35–38] In the case here, the sequence lengths between the two target sites are relatively short as compared to the nascent mRNA length of more than 28,000 bases; target sites from ISS-N1 to ISS+100 ≤ 65 bases and from ISS-N1 to 3′ splice site of exon 8 ≤ 410 bases. Therefore, a dual-targeting AON may increase the likelihood of masking both target elements simultaneously due to cooperative binding. That is, binding to the first target site could bring the dual-targeting AON near the other target site for the second binding event. This possibility is not apparent in single-targeting AONs. Nevertheless, not every molecule of the dual-targeting AONs will bind to two target sites simultaneously and some transcripts may have one AON bound to each target site. In this scenario, the advantages of dual-targeting AONs are negated. At 200 nmol/l, Dual-2 is 19% more efficient than the combination of N1-2 and ex8-2 (**Supplementary Figure S5**). It will be interesting and of translational value to validate the superiority of dual-targeting AONs in future studies through comparisons of more dual-targeting AONs with their corresponding mixture of single-targeting AONs over a wide range of AON concentrations.

As there are more than 100,000 splicing decisions occurring in a human cell,[39] the complexity in the regulation of *SMN2* exon 7 splicing is likely to be a common phenomenon.[40,41] The use of AON to mask a specific SRE is an apt approach to investigate the influence of each SRE on the modulation of exon splicing. The key advantage over mutational studies using minigenes and competitive dosing of splicing proteins is it minimizes disruptions to the gene of study and the whole cell's splicing process. In particular, negative SREs can be masked by AONs to study inhibition of exon inclusion whereas positive SREs can be targeted to study inhibition of exon skipping.

METHODS AND MATERIALS

Cell culture. Fibroblast cell line (GM03813) derived from a human donor with SMA type I and having two copies of the *SMN2* gene, hereafter termed as SMA fibroblast cells, was obtained from Coriell (Camden, NJ) and used in transfection studies of the AONs. The SMA fibroblast cells were grown in Basal Fibroblast Medium (Promocell, Heidelberg, Germany) containing basic fibroblast growth factor and insulin, with 15% feral calf serum, 2 mmol/l L-Glutamine, 10% Penicillin/Streptomycin.

Transfection. AON transfection was performed using reagents according to the manufacturer's recommendations. In brief, 5 µl of Lipofectamine2000 (Invitrogen, Carlsbad, CA) was added to a round bottom tube and 95 µl of Opti-Mem reduced serum medium (Invitrogen). Ninety-eight microlitre of Opti-Mem reduced serum medium was mixed with 2 µl of AON in an eppendorf tube and allowed to stand for 5 minutes. This mixture was then added to the contents of the round bottom tube, mixed and allowed to stand for 30 minutes. This solution was topped up to 2 ml with Opti-Mem I reduced serum medium with 5% serum (*i.e.*, the "transfection mixture"). To evaluate AON dose effect, transfection was carried out with AON concentrations of 25 nmol/l, 50 nmol/l, 100 nmol/l, and 200 nmol/l in the total of transfection mixture.
Twenty-four hours prior to transfection, the SMA fibroblast cells were seeded into 6 well plates. On the day of transfection, the cells were at a density of ~80%. After removal of culture medium, 2 ml aliquots of the transfection mixture containing the AON were added to separate wells and incubated for 5 hours. Thereafter, the transfection mixture was replaced by cell culture medium. Cells were harvested for RNA extraction at 24 hours, followed by total RNA extraction, reverse transcription polymerase chain reaction (RT-PCR) and Quantitative Real-time PCR (qPCR) to quantitate exon 7 inclusion.

RNA extraction. RNA was extracted using the Nucleospin RNA II kit (Macherey-Nagel, Düren, Germany) according to the manufacturer's recommendations. RNA concentration was measured with Nanodrop (Thermo Scientific, Wilmington, DE).

Reverse transcription polymerase chain reaction. Reverse transcription was performed with a SuperScript III cDNA synthesis kit (Invitrogen) according to the manufacturer's protocol, using an oligo(dT) primer. Primers for the PCR were: exon 6 forward primer 5′-accacctcccatatgtccag-3′ and exon 8 reverse primer 5′-tttgaagaaatgaggccagtt-3′. PCR cycling conditions were: 94 °C for 5 minutes; 35 cycles of 94 °C for 30 seconds (denaturation); 60 °C for 30 seconds (annealing); 72 °C for 1 minute (extension); 72 °C for 10 minutes and hold at 4 °C. The PCR amplicons were separated by standard gel electrophoresis. Image software was used for densitometry analysis of the separated PCR amplicons.

Quantitative Real-time PCR (qPCR) to evaluate dose effect of AON transfection concentration. Primers for the qPCR were: forward primer 5′-aatcaaaaagaaggaaggtgct-3′ corresponding a segment in exon 7 and reverse primer 5′- tttgaagaaatgaggccagtt-3′ corresponding to a segment in exon 8. The qPCR reaction mixture was prepared in optical tubes using the Roche Light Cycler DNA Master Plus Mix (Indianapolis, IN). The PCR was performed on a BioRad CFX96 Real Time PCR machine (Hercules, CA) with the cycling conditions: 94 °C 4 minutes; 38 cycles of 95 °C for 10 seconds (denaturation); 60 °C for 10 seconds (annealing), primer extension at 72 °C for 10 seconds (extension). Melting curve was performed from 65 °C to 95 °C. qPCR specificity was confirmed by 2% agarose gel using 10 µl of qPCR product. qPCRs were performed in triplicates for each AON treatment trial.

Protein extraction and western blotting. Upon AON transfection, cells were lysed with lysis buffer containing protease inhibitor cocktail (Promega, Fitchburg, WI) according to the manufacturer's instructions. The average concentration of protein in each sample was determined using the Bradford protein quantification method. The proteins in the samples were separated on 12% SDS-PAGE and electroblotted onto nitrocellulose membranes.
The membranes were probed for SMN protein with monoclonal anti-SMN antibody (BD Transduction Laboratories, San Jose, CA) at 1:1,000

dilution as the primary antibody. Monoclonal anti-α-tubulin antibody (Sigma, St Louis, MO) at 1:10,000 dilution was used to probe α-tubulin as a control. The secondary antibody was horseradish peroxidase-conjugated goat anti-mouse polyclonal antibody (BioRad, Hercules, CA) at a dilution of 1:5,000. Detection was performed with the ECL western blotting detection reagents (GE Healthcare, Pittsburgh, PA) and ECL Hyper film (GE Healthcare). Densitometry analysis of the protein bands was performed using ImageJ software.

Immunofluorescence and Nuclear GEM quantification. SMA fibroblast cells were plated onto four chamber slides and transfected separately with various 100 nmol/l of AONs as described above. At 48 hours after addition of the transfection mixture, the cells were washed in phosphate-buffered saline, fixed with 4% paraformaldehyde for 15 minutes, blocked with 1 mg/ml bovine serum albumin and incubated with monoclonal anti-SMN antibody (BD Transduction Laboratories) as the primary anti-SMN antibody at a dilution of 1:50 or 1:100. The cells were washed to remove unbound antibody before incubation with secondary antibody Alexa Fluor 594 conjugated goat anti-mouse antibody (Invitrogen) at a dilution of 1:1,000. Nuclei were counterstained with DAPI. The cells were washed again and examined under confocal laser-scanning microscope Nikon A1 (Japan) for Gemini of coiled body (GEMs) counting. For each AON transfection, 120 consecutive cells were counted to determine the number of nuclear GEMs per cell while disregarding cytoplasmic GEMs.

A fibroblast cell line from a healthy SMA carrier individual (GM05758), also from Coriell, was also cultured for use as a control in the immunohistochemical studies. The cells were grown in DMEM with 15% feral calf serum, 2 mmol/l L-Glutamine, 10% Penicillin/Streptomycin.

SUPPLEMENTARY MATERIALS

Figure S1. Percentage of amplicons with exon 7 inclusion estimated by densitometry analysis of inefficient AONs

Figure S2. Representative immunofluorescence stained cells

Figure S3. Table for nuclear GEMs counts

Figure S4. Comparison of fold increase of full-length *SMN* transcripts induced by dual-targeting AONs with their respective single-targeting AONs

Figure S5. Comparison of the efficiency of Dual-2 versus mixture of N1-2 and ex8-2

REFERENCES

1. Lefebvre, S, Bürglen, L, Reboullet, S, Clermont, O, Burlet, P, Viollet, L *et al.* (1995). Identification and characterization of a spinal muscular atrophy-determining gene. *Cell* **80**: 155–165.
2. Lorson, CL, Hahnen, E, Androphy, EJ and Wirth, B (1999). A single nucleotide in the SMN gene regulates splicing and is responsible for spinal muscular atrophy. *Proc Natl Acad Sci USA* **96**: 6307–6311.
3. Cartegni, L and Krainer, AR (2002). Disruption of an SF2/ASF-dependent exonic splicing enhancer in SMN2 causes spinal muscular atrophy in the absence of SMN1. *Nat Genet* **30**: 377–384.
4. Kashima, T and Manley, JL (2003). A negative element in SMN2 exon 7 inhibits splicing in spinal muscular atrophy. *Nat Genet* **34**: 460–463.
5. Singh, NN, Androphy, EJ and Singh, RN (2004). *In vivo* selection reveals combinatorial controls that define a critical exon in the spinal muscular atrophy genes. *RNA* **10**: 1291–1305.
6. Lorson, CL and Androphy, EJ (2000). An exonic enhancer is required for inclusion of an essential exon in the SMA-determining gene SMN. *Hum Mol Genet* **9**: 259–265.
7. Feldkötter, M, Schwarzer, V, Wirth, R, Wienker, TF and Wirth, B (2002). Quantitative analyses of SMN1 and SMN2 based on real-time lightCycler PCR: fast and highly reliable carrier testing and prediction of severity of spinal muscular atrophy. *Am J Hum Genet* **70**: 358–368.
8. McAndrew, PE, Parsons, DW, Simard, LR, Rochette, C, Ray, PN, Mendell, JR *et al.* (1997). Identification of proximal spinal muscular atrophy carriers and patients by analysis of SMNT and SMNC gene copy number. *Am J Hum Genet* **60**: 1411–1422.
9. Wirth, B, Brichta, L, Schrank, B, Lochmüller, H, Blick, S, Baasner, A *et al.* (2006). Mildly affected patients with spinal muscular atrophy are partially protected by an increased SMN2 copy number. *Hum Genet* **119**: 422–428.
10. Singh, NN, Singh, RN and Androphy, EJ (2007). Modulating role of RNA structure in alternative splicing of a critical exon in the spinal muscular atrophy genes. *Nucleic Acids Res* **35**: 371–389.
11. Lim, SR and Hertel, KJ (2001). Modulation of survival motor neuron pre-mRNA splicing by inhibition of alternative 3′ splice site pairing. *J Biol Chem* **276**: 45476–45483.
12. Hua, Y, Vickers, TA, Baker, BF, Bennett, CF and Krainer, AR (2007). Enhancement of SMN2 exon 7 inclusion by antisense oligonucleotides targeting the exon. *PLoS Biol* **5**: e73.
13. Hua, Y, Vickers, TA, Okunola, HL, Bennett, CF and Krainer, AR (2008). Antisense masking of an hnRNP A1/A2 intronic splicing silencer corrects SMN2 splicing in transgenic mice. *Am J Hum Genet* **82**: 834–848.
14. Madocsai, C, Lim, SR, Geib, T, Lam, BJ and Hertel, KJ (2005). Correction of SMN2 Pre-mRNA splicing by antisense U7 small nuclear RNAs. *Mol Ther* **12**: 1013–1022.
15. Pramono, ZA, Wee, KB, Wang, JL, Chen, YJ, Xiong, QB, Lai, PS *et al.* (2012). A prospective study in the rational design of efficient antisense oligonucleotides for exon skipping in the DMD gene. *Hum Gene Ther* **23**: 781–790.
16. Wee, KB, Pramono, ZA, Wang, JL, MacDorman, KF, Lai, PS and Yee, WC (2008). Dynamics of co-transcriptional pre-mRNA folding influences the induction of dystrophin exon skipping by antisense oligonucleotides. *PLoS ONE* **3**: e1844.
17. Coovert, DD, Le, TT, McAndrew, PE, Strasswimmer, J, Crawford, TO, Mendell, JR *et al.* (1997). The survival motor neuron protein in spinal muscular atrophy. *Hum Mol Genet* **6**: 1205–1214.
18. Miyaso, H, Okumura, M, Kondo, S, Higashide, S, Miyajima, H and Imaizumi, K (2003). An intronic splicing enhancer element in survival motor neuron (SMN) pre-mRNA. *J Biol Chem* **278**: 15825–15831.
19. Singh, NK, Singh, NN, Androphy, EJ and Singh, RN (2006). Splicing of a critical exon of human Survival Motor Neuron is regulated by a unique silencer element located in the last intron. *Mol Cell Biol* **26**: 1333–1346.
20. Porensky, PN, Mitrpant, C, McGovern, VL, Bevan, AK, Foust, KD, Kaspar, BK *et al.* (2012). A single administration of morpholino antisense oligomer rescues spinal muscular atrophy in mouse. *Hum Mol Genet* **21**: 1625–1638.
21. Osman, EY, Yen, PF and Lorson, CL (2012). Bifunctional RNAs targeting the intronic splicing silencer N1 increase SMN levels and reduce disease severity in an animal model of spinal muscular atrophy. *Mol Ther* **20**: 119–126.
22. Passini, MA, Bu, J, Richards, AM, Kinnecom, C, Sardi, SP, Stanek, LM *et al.* (2011). Antisense oligonucleotides delivered to the mouse CNS ameliorate symptoms of severe spinal muscular atrophy. *Sci Transl Med* **3**: 72ra18.
23. Hua, Y, Sahashi, K, Rigo, F, Hung, G, Horev, G, Bennett, CF *et al.* (2011). Peripheral SMN restoration is essential for long-term rescue of a severe spinal muscular atrophy mouse model. *Nature* **478**: 123–126.
24. Singh, NN, Shishimorova, M, Cao, LC, Gangwani, L and Singh, RN (2009). A short antisense oligonucleotide masking a unique intronic motif prevents skipping of a critical exon in spinal muscular atrophy. *RNA Biol* **6**: 341–350.
25. Baughan, TD, Dickson, A, Osman, EY and Lorson, CL (2009). Delivery of bifunctional RNAs that target an intronic repressor and increase SMN levels in an animal model of spinal muscular atrophy. *Hum Mol Genet* **18**: 1600–1611.
26. Singh, NN, Seo, J, Ottesen, EW, Shishimorova, M, Bhattacharya, D and Singh, RN (2011). TIA1 prevents skipping of a critical exon associated with spinal muscular atrophy. *Mol Cell Biol* **31**: 935–954.
27. Hofmann, Y, Lorson, CL, Stamm, S, Androphy, EJ and Wirth, B (2000). Htra2-beta 1 stimulates an exonic splicing enhancer and can restore full-length SMN expression to survival motor neuron 2 (SMN2). *Proc Natl Acad Sci USA* **97**: 9618–9623.
28. Hofmann, Y and Wirth, B (2002). hnRNP-G promotes exon 7 inclusion of survival motor neuron (SMN) via direct interaction with Htra2-beta1. *Hum Mol Genet* **11**: 2037–2049.
29. Young, PJ, DiDonato, CJ, Hu, D, Kothary, R, Androphy, EJ and Lorson, CL (2002). SRp30c-dependent stimulation of survival motor neuron (SMN) exon 7 inclusion is facilitated by a direct interaction with hTra2 beta 1. *Hum Mol Genet* **11**: 577–587.
30. Helmken, C, Hofmann, Y, Schoenen, F, Oprea, G, Raschke, H, Rudnik-Schöneborn, S *et al.* (2003). Evidence for a modifying pathway in SMA discordant families: reduced SMN level decreases the amount of its interacting partners and Htra2-beta1. *Hum Genet* **114**: 11–21.
31. Gladman, JT and Chandler, DS (2009). Intron 7 conserved sequence elements regulate the splicing of the SMN genes. *Hum Genet* **126**: 833–841.
32. Mayeda, A and Krainer, AR (1992). Regulation of alternative pre-mRNA splicing by hnRNP A1 and splicing factor SF2. *Cell* **68**: 365–375.
33. Kashima, T, Rao, N and Manley, JL (2007). An intronic element contributes to splicing repression in spinal muscular atrophy. *Proc Natl Acad Sci USA* **104**: 3426–3431.
34. Singh, RN (2007). Evolving concepts on human SMN pre-mRNA splicing. *RNA Biol* **4**: 7–10.
35. Eperon, LP, Graham, IR, Griffiths, AD and Eperon, IC (1988). Effects of RNA secondary structure on alternative splicing of pre-mRNA: is folding limited to a region behind the transcribing RNA polymerase? *Cell* **54**: 393–401.
36. Nowakowski, J, Shim, PJ, Prasad, GS, Stout, CD and Joyce, GF (1999). Crystal structure of an 82-nucleotide RNA-DNA complex formed by the 10-23 DNA enzyme. *Nat Struct Biol* **6**: 151–156.
37. Kramer, FR and Mills, DR (1981). Secondary structure formation during RNA synthesis. *Nucleic Acids Res* **9**: 5109–5124.
38. Repsilber, D, Wiese, S, Rachen, M, Schröder, AW, Riesner, D and Steger, G (1999). Formation of metastable RNA structures by sequential folding during transcription: time-resolved structural analysis of potato spindle tuber viroid (-)-stranded RNA by temperature-gradient gel electrophoresis. *RNA* **5**: 574–584.
39. Nilsen, TW and Graveley, BR (2010). Expansion of the eukaryotic proteome by alternative splicing. *Nature* **463**: 457–463.
40. Pagani, F, Raponi, M and Baralle, FE (2005). Synonymous mutations in CFTR exon 12 affect splicing and are not neutral in evolution. *Proc Natl Acad Sci USA* **102**: 6368–6372.
41. López-Bigas, N, Audit, B, Ouzounis, C, Parra, G and Guigó, R (2005). Are splicing mutations the most frequent cause of hereditary disease? *FEBS Lett* **579**: 1900–1903.
42. Miyajima, H, Miyaso, H, Okumura, M, Kurisu, J and Imaizumi, K (2002). Identification of a cis-acting element for the regulation of SMN exon 7 splicing. *J Biol Chem* **277**: 23271–23277.
43. Monani, UR, Lorson, CL, Parsons, DW, Prior, TW, Androphy, EJ, Burghes, AH *et al.* (1999). A single nucleotide difference that alters splicing patterns distinguishes the SMA gene SMN1 from the copy gene SMN2. *Hum Mol Genet* **8**: 1177–1183.
44. Dickson, A, Osman, E and Lorson, CL (2008). A negatively acting bifunctional RNA increases survival motor neuron both *in vitro* and in vivo. *Hum Gene Ther* **19**: 1307–1315.